metals

MDPI

Article

A Comparison Study of Fatigue Behavior of S355J2+N, S690QL and X37CrMoV5-1 Steel

Vladimir Milovanović [1], Dušan Arsić [1], Miroslav Milutinović [2,*], Miroslav Živković [1] and Marko Topalović [3]

[1] University of Kragujevac, Faculty of Engineering, 34000 Kragujevac, Serbia; vladicka@kg.ac.rs (V.M.); dusan.arsic@fink.rs (D.A.); zile@kg.ac.rs (M.Ž.)
[2] University of East Sarajevo, Faculty of Mechanical Engineering, 71123 East Sarajevo, Bosnia and Herzegovina
[3] University of Kragujevac, Institute for Information Technologies, 34000 Kragujevac, Serbia; topalovic@kg.ac.rs
* Correspondence: miroslav.milutinovic@ues.rs.ba

Abstract: Steel of the mild-strength S355J2+N steel grade is the most often used steel for manufacturing carrying sections of constructions exposed to fatigue loads. The use of high-strength steels, such as S690QL, allows for the creation of structures that are light and simple to construct. However, increasing the yield strength of high-strength steels does not result in a corresponding increase in fatigue resistance. As a result, using high-strength steels for constructions subjected to fatigue loading can be a major design concern, raising the question of whether high-strength steels should be used at all. Most of the experimental investigations regarding the hot work tool steel X37CrMoV5-1 found in the literature are focused on its machining and wear resistance, with insufficient attention paid to the cyclic loads. This article evaluates the fatigue properties of mild-strength S355J2+N, high-strength S690QL, and X37CrMoV5-1 steel grades. A SHIMADZU servo-hydraulic testing machine is used to perform uniaxial tensile tests under uniaxial fatigue stress-controlled, fully reversed conditions (tensile–compression testing with $R = -1$ stress ratio) in accordance with EN ISO and ASTM standards. The aim of this paper is to highlight the fatigue characteristics of these three steels that are among the most used in their respective groups. Steel S355J2+N belongs to the group of hot-rolled normalized steels, S690QL belongs to the group of improved (quenched + tempered) steels with increased strength, and X37CrMoV5-1 belongs to the group of high-alloyed tool steels for hot work. This choice was made as the tested steels can be considered typical representatives of their groups. Based on the test results of these three steels, which are organized in *S–N* curves, the fatigue behavior of the entire mentioned groups of steels can be foreseen.

Keywords: structural fatigue tests; fatigue life; *S–N* fatigue curves; S355J2+N steel grade; S690QL steel grade; STRENX 700 steel grade; X37CrMoV5-1 steel grade; AISI H11 steel grade

Citation: Milovanović, V.; Arsić, D.; Milutinović, M.; Živković, M.; Topalović, M. A Comparison Study of Fatigue Behavior of S355J2+N, S690QL and X37CrMoV5-1 Steel. *Metals* **2022**, *12*, 1199. https://doi.org/10.3390/met12071199

Academic Editors: Jai-Won Byeon and Jae-Yeon Kim

Received: 17 June 2022
Accepted: 11 July 2022
Published: 14 July 2022

1. Introduction

Despite the development of new alloys [1] and composite materials [2], steels are still the most widely utilized materials in mechanical [3] and civil engineering [4]. Steel structural elements and constructions are frequently subjected to varying loads over their service (fatigue) lives [5,6]. Due to the nature of their sufficient qualities and inexpensive prices, structural steels S235 [7], S275 [8], and S355 [9,10] are the most extensively used steels for structural elements and constructions exposed to fatigue stress [11]. High-strength steel [12] is used in order to meet the requirements for light constructions with simple designs while having excellent structural performance.

The *S–N* curves proposed in the design regulations EN 1993-1-9 [13] and EN 13001-3-1 [14] do not reveal the exact material dependence; hence, the exact fatigue properties of different steel types must be determined. In general, the fatigue behavior of structural steels is well-understood and investigated by many researchers [9,10,15], but high-strength

steels are still understudied, and determining their mechanical properties (fatigue) has become the particular focus of several researchers [16–19].

Experimental testing of steel is unavoidable and crucial in fatigue life prediction as different specimens made of the same material can have different impurities, non-metallic inclusions, and slightly different compositions of alloying elements, which, depending on the steel grade, can scatter results significantly.

Fatigue life prediction is a field gaining considerable attention in material science, and multiaxial fatigue models [20], which can be based on stress, strain, energy, or fracture mechanics [21], are utilized. Each of these approaches is suitable for specific loading conditions; for instance, stress-based models are the most appropriate for high cycle fatigue (such as the one presented in this paper), while strain-based models are better suited for low cycle fatigue in which plastic deformation is notable [21]. Energy-based models consider both contributions from stress and strain and can predict the reduction in fatigue life due to the out-of-phase hardening [21], while the Strain Energy Density-based (SED) fatigue model can predict ratcheting phenomena [22]. Based on the experimental analysis of crack formation and growth studied in the fracture mechanics field, the critical plane method is used to predict ductile or brittle failure [21]. The maximum normal stress range plane is used to predict brittle failure, and the maximum shear stress range plane is applied to estimate ductile failure [21]. This analysis requires notched specimens and a high-resolution camera with an optical device with variable magnification [23]. Another similar issue is the requirement of servo-hydraulic machines that can perform multiaxial loading (including torsion); hence, researchers often propose the extrapolation of data obtained using a uniaxial test [20–23]. In fact, in [20], the authors determined most of the coefficients using a monotonic tensile test, while the authors in [23] used two uniaxial fully reversed strain-controlled tests, one with a higher strain amplitude and another with a lower strain amplitude, to evaluate the strain–life relationship and two elastic–plastic numerical models, which they used to complement the experimental data. In this paper, we present our contribution to the field of fatigue damage assessment of high-strength steels, which complements existing research and provides engineers with valuable data that will facilitate new lightweight construction designs. The fatigue characteristics of the high-strength steel grade S690QL, also known as STRENX 700 (according to manufacturer SSAB Corporation, Stockholm, Sweden), in the gigacycle region of loading are presented in [24]. However, the experiments presented in [24] are conducted at the high-frequency loading of $f \approx 20$ kHz, which is unrealistic for the most real-life steel constructions. The ultrasonic impact treatment of welded joints made of S690QL steel is studied in [25]. This treatment increases the fatigue limit at $N = 10^7$ cycles and at the testing frequency of $f = 35$ Hz by about 12% [25]. In our research, we use even lower frequencies of 10 and 15 Hz for up to $N = 2 \times 10^6$ cycles on untreated material, filling the gap between [24] and [25].

The hot work tool steel X37CrMoV5-1, also known as H11 [26], according to the American Iron and Steel Institute (AISI), is used primarily for making tools for the die casting of aluminum alloys, copper, plastic, and other materials. It has high thermal fatigue [26] and wear resistance [27], and it is suitable for the machining processing [28]. In the literature, hot work tool steels are usually tested to withstand low cycle fatigue [29], which is, of course, in accordance with their purpose [26]. However, in this paper, we present the experimental fatigue testing of X37CrMoV5-1 with $N = 2 \times 10^6$ cycles, the same as the two other steel grades, in order to carry out a corresponding comparison between them. This addresses the feasibility of expanding X37CrMoV5-1 implementation for the construction of parts and constructions subjected to long-lasting fatigue loads and provides engineers with the appropriate data for designing such elements.

The remainder of the paper is organized as follows: in the Materials and Methods Section, a theoretical background of fatigue behavior analysis is given, followed by an experimental setup description. This includes a description of the chemical composition of the tested materials and specimen dimensions, as well as a description of the testing machine and equipment. References to related standards are also given. The Results Section

is dedicated to the presentation of the *S–N* curve charts and fatigue strengths given in tables. The Discussion Section features a comparison between the tested steels and the possible implications of the obtained results on mechanical parts and construction design. In the Conclusion, we point out that although S355J2+N has a significant strain hardening, while S690QL and X37CrMoV5-1 steel have only minor strain hardening, the reduction in the dimension of structural elements made using high-strength steels can lead to the elevation of the fatigue sensitivity in these elements.

2. Materials and Methods

2.1. Fatigue Behavior Assessment

Fatigue tests evaluate a material's resistance to damage, loss of strength, and failure when subjected to cyclical loading. The fatigue test approaches are classified into *S–N* and *ε–N* linear fracture mechanics approaches as classical approaches, and the increasingly popular energy-based approaches. Equation (1) [30,31], Equation (2) [31,32], and Equation (3) [31,33] shown below are the most well-known relationships for describing fatigue behavior:

$$\frac{\Delta\sigma}{2} = \sigma_a = \sigma'_f \left(2N_f\right)^b, \tag{1}$$

$$\frac{\Delta\varepsilon_p}{2} = \varepsilon'_f \left(2N_f\right)^c, \tag{2}$$

$$\varepsilon_a = \frac{\Delta\varepsilon}{2} = \varepsilon_{a,e} + \varepsilon_{a,p} = \frac{\Delta\varepsilon_e}{2} + \frac{\Delta\varepsilon_p}{2} = \frac{\sigma'_f}{E}\left(2N_f\right)^b + \varepsilon'_f \left(2N_f\right)^c. \tag{3}$$

In Equations (1)–(3) σ_a is the true stress amplitude, and $2N_f$ is the number of reversals to failure. The fatigue strength coefficient is denoted with σ'_f and the fatigue strength exponent with b. The fatigue ductility coefficient is given with ε'_f and the fatigue ductility exponent with c. ε_a, $\varepsilon_{a,e}$, $\varepsilon_{a,p}$ are the total, elastic, and plastic strain amplitudes, respectively. E is the Young's modulus. The commonly known stress–life (*S–N*) approach, based on the Basquin model [30] specified in Equation (1), was used to determine the fatigue properties of the studied materials (S355J2+N, S690QL, and X37CrMoV5-1). The *S–N* approach is a global strategy that is related to the stress range, and it is the foundation of several fatigue life standards, such as Eurocode 3, part 1–9 [32]. Given the fact that there is only one stress component in most fatigue life calculations, the math is relatively simple. The results of the *S–N* approach show a clear relationship between a global definition of the stress range (stress amplitude) and the total number of reversals to failure. The Basquin equation (Equation (1)) is often adopted for representing the Wöhler curve [34] as a straight line in a double logarithmic plot.

2.2. Basic Properties of Studied Steels

Mild-strength S355J2+N steel, high-strength S690QL steel, and hot work tool steel grade X37CrMoV5-1 steel were used for this experimental study. A comparison of the chemical composition (in terms of weight %) of these steels [35–38] was obtained using spark emission spectrometry and is shown in Table 1. The S355J2+N and S690QL steels are suitable for welding; however, due to the higher amount of alloy elements, the weldability of high-strength steels is often less than that of mild-strength steel. On the other hand, X37CrMoV5-1 has poor weldability but good machinability.

Table 1. Comparison of the chemical composition of the S355J2+N, S690QL, and X37CrMoV5-1 steel grades (weight %).

Steel Grade	C	Si	Mn	P	S	Cr	Ni
S355J2+N	0.161	0.046	1.488	0.0224	0.0086	0.040	0.014
S690QL	0.11	0.093	0.64	0.009	0.017	-	-
X37CrMoV5-1	0.37	1.0	0.4	<0.03	<0.02	5.2	-
Steel grade	Mo	Cu	N	Al	Nb	V	Ti
S355J2+N	0.05	0.005	0.004	0.049	-	-	-
S690QL	-	-	-	0.017	0.088	0.19	0.14
X37CrMoV5-1	1.2	-	-	-	-	0.4	-

The specimens used to determine and validate the static strength properties of the three steel grades used in the experimental program were prepared according to the standards EN ISO 6892-1 [39] and ASTM E8M-01 [40]. Uniaxial tensile tests were performed on three representative flat specimens for each steel, with the same thickness in all cross-sections to investigate the static strength properties.

The technical drawing and real shape of one of the investigated specimens, before testing, is shown in Figure 1. All nominal dimensions of the specimen shown in Figure 1 are in millimeters (mm).

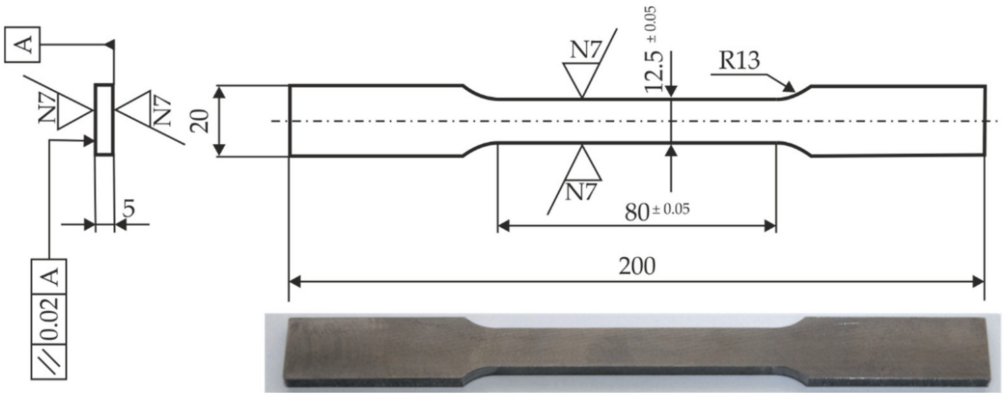

Figure 1. Technical drawing of testing specimen and real specimen (unit: mm).

The uniaxial tensile tests on the specimens to determine their static strength properties (mechanical characteristics) were performed using a SHIMADZU type EHF EV101K3-070-0A servo-hydraulic testing machine (Shimadzu Corporation, Tokyo, Japan) with a force of ±100 kN and a stroke of ±100 mm (Figure 2).

The uniaxial tensile tests were carried out in accordance with EN ISO 6892-1 [39] and ASTM E8M-01 [40] at room temperature (23 ± 5 °C) with a constant stroke control rate of 4 mm/min (strain rate 10^{-3} s^{-1}) without a change in the speed of testing. One of the investigated specimens (S355J2+N steel grade) at the end of the uniaxial tensile test is presented in Figure 3a. An MFA25 extensometer (MF Mess & Feinwerktechnik GmbH, Velbert, Germany) with a gauge length of 50 mm was used to determine the Young's modulus and elongation, and it is shown in Figure 3b.

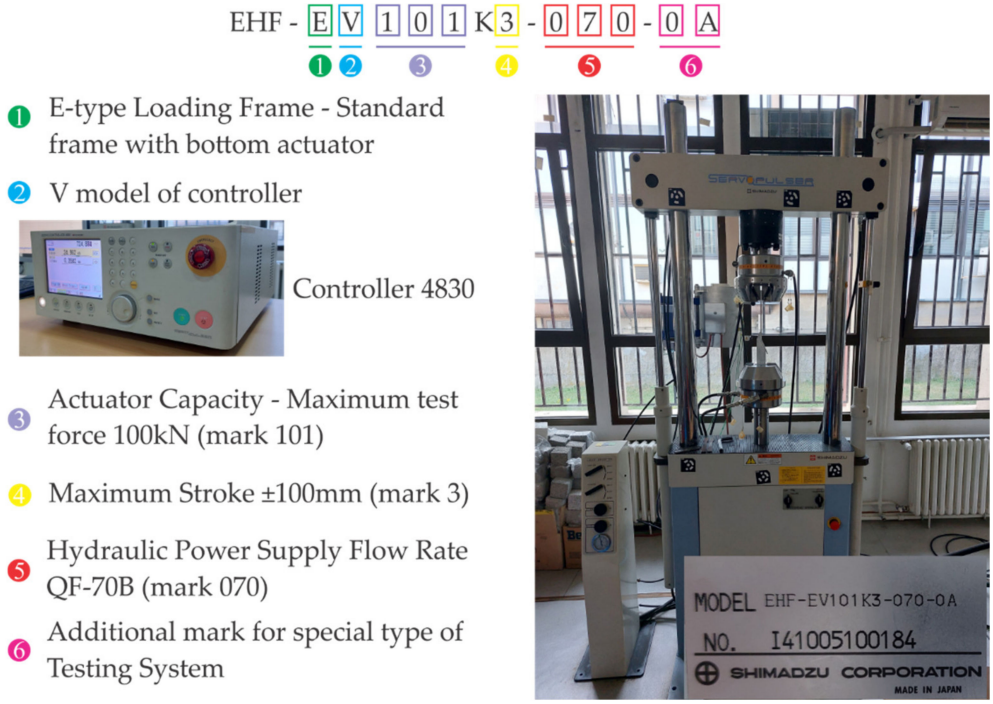

Figure 2. SHIMADZU servo-hydraulic machine.

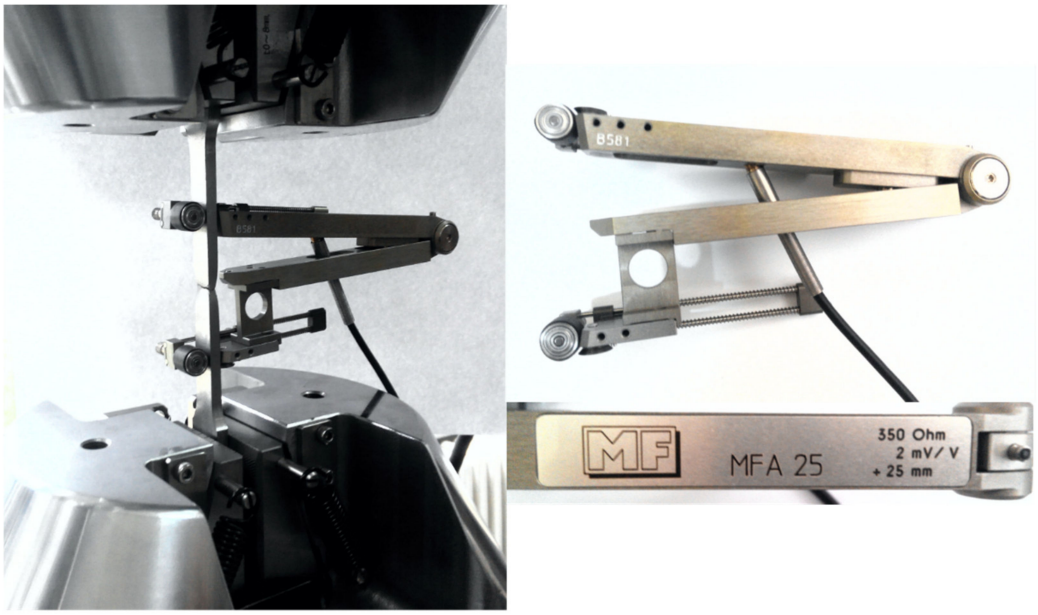

Figure 3. Testing equipment: (**a**) SHIMADZU servo-hydraulic machine, (**b**) MFA25 extensometer.

As an outcome of the uniaxial tensile tests on the three flat specimens, for each steel, we determined the mechanical characteristics of the S355J2+N, S690QL, and X37CrMoV5-1 steel grades. The average yield strength, tensile strength, and Young's modulus for each steel are shown in Table 2.

Table 2. Mechanical characteristics of S355J2+N, S690QL, and X37CrMoV5-1.

Steel Grade	Yield Strength σ_y (MPa)	Tensile Strength σ_u (MPa)	Young's Modulus E (GPa)	Tensile Strain-Hardening Exponent n (-)	Strength Coefficient K (MPa)
S355J2+N	401.24	539.36	206.26	0.2129	920.49
S690QL	767.97	818.08	228.89	0.0509	992.67
X37CrMoV5-1	1499	1687	218	0.01667	1961.3

The force–displacement responses were recorded for all tested specimens, and the response of "Specimens with results close to average values of mechanical characteristics" was selected as the representative for the determination of the tensile strain-hardening exponent, n, and strength coefficient, K, according to ASTM E646-00 [41], for each tested steel grade.

Another result of the conducted uniaxial tensile testing is the stress–strain curves for the S355J2+N, S690QL, and X37CrMoV5-1 steel grades that are shown in Figure 4 for one of the representative specimens (a specimen with results close to the average values of the mechanical characteristics) for each investigated steel.

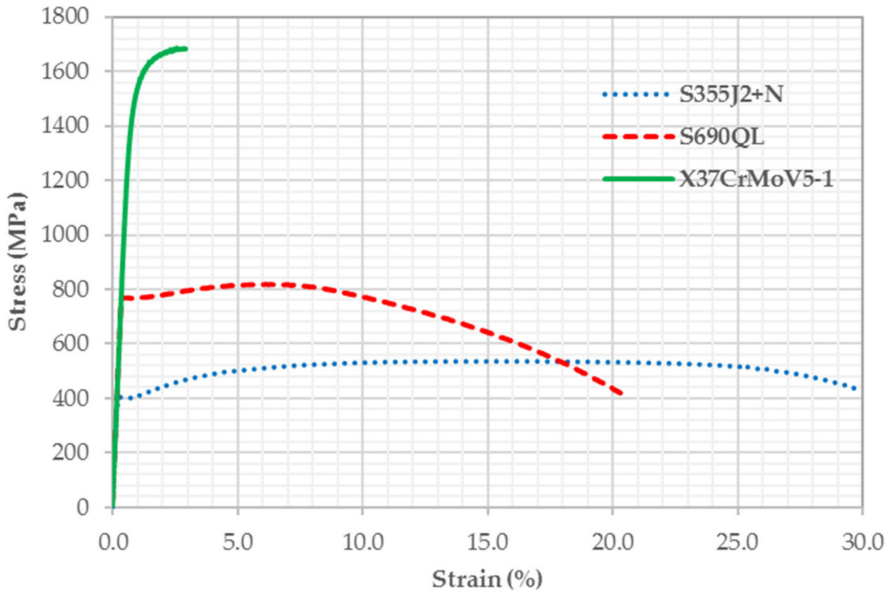

Figure 4. Stress–strain curves for S355J2+N, S690QL, and X37CrMoV5-1 steel grades.

2.3. Fatigue Analysis Using the Experimental Method

This section describes a complete fatigue characterization of mild-strength S355J2+N steel, high-strength S690QL steel, and hot work tool steel grade X37CrMoV5-1 steel, carried out according to the internal procedures of the Centre for Engineering Software and Dynamic Testing at the Faculty of Engineering University of Kragujevac using a SHIMADZU type EHF EV101K3-070-0A servo-hydraulic testing machine (Shimadzu Corporation, Tokyo, Japan) with a force of ±100 kN and a stroke of ±100 mm, based on ASTM E468-90 [42].

All specimens utilized to determine the fatigue properties of each steel were prepared according to the standard E468-90 [42]. The technical drawing and real shape of one of the investigated specimens for fatigue testing, before testing, is shown in Figure 5. All nominal dimensions of the specimen shown in Figure 5 are in millimeters (mm). All specimens were finely polished to minimize surface roughness effects. The mean roughness level achieved on the surface of the gauge length of the specimens was in the range of 1–5 μm after polishing. To calculate the roughness measurement the SJ-210 Portable Surface Roughness Tester (Mitutoyo America Corporation, Aurora, IL, USA) was used.

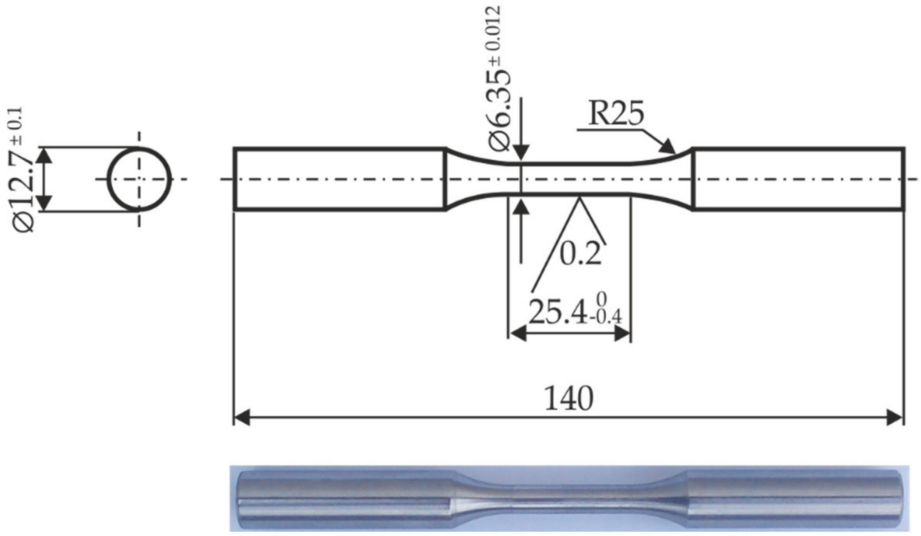

Figure 5. Technical drawing of fatigue testing specimen and real specimen (unit: mm).

One series of 15 specimens was prepared for each steel. Uniaxial tension–compression fatigue tests were performed by applying a sinusoidal wave on the SHIMADZU servo-hydraulic testing machine (Shimadzu Corporation, Tokyo, Japan). The specimens were exposed to high cycle fatigue under stress-controlled, fully reversed (tensile-compression) testing conditions in accordance with ASTM E468-90 [42]. The stress ratio for all tested specimens was $R = -1$. The stress levels used to control the fatigue tests were chosen from the previously performed monotonic uniaxial tensile test described in Section 2.2.

For mild-strength S355J2+N steel and high-strength S690QL steel, 6 levels of stress amplitude were used for fatigue testing. We had three repetitions per level with a high range of stress amplitude and two repetitions per level with a low range of stress amplitude.

Given the scatter in the data obtained during the testing of the specimens of the hot work tool steel grade X37CrMoV5-1, 4 levels of stress amplitude were used for fatigue testing. We conducted three and four repetitions per two level stress amplitude in order to obtain a better repetition of results.

During the testing of fatigue properties, the frequency was 10 or 15 Hz, and complete failure of the specimen was used as a criterion for the test stop.

3. Results

The initial uniaxial tensile testing gave us the stress–strain curves shown in Figure 4. Based on these curves, we could compare the yield region of all steels and observe the initial strain hardening behavior of the S355J2+N steel. It is clear that the S355J2+N steel shows a yield plateau, after which a very significant strain hardening can be verified. The S690QL steel does not show that yield plateau, and a relatively small strain hardening can be observed. The X37CrMoV5-1 steel has a significantly higher limit of proportionality, as can be seen in Figure 4, but it yields at less than 3% strain.

Therefore, we chose different stress amplitudes for each steel grade in order to cover a wide range of cyclic load conditions. For S355J2+N, we used amplitudes between 200 and 350 MPa; for S690QL, we used amplitudes between 300 and 540 MPa; and for X37CrMoV5-1, we used amplitudes between 500 and 1000 MPa. The common amplitude for S355J2+N and S690QL is 350 MPa, and for S690QL and X37CrMoV5-1, it is 500 MPa.

Table 3. S355J2+N, S690QL, and X37CrMoV5-1 fatigue test results under stress-controlled conditions.

Steel Grade	**S355J2+N**		
Specimen Designation	**Stress Amplitude σ_a (MPa)**	**Frequency (Hz)**	**Number of Cycles to Failure N_f**
1	350	10	12,843
2	350	10	14,564
3	350	10	18,394
4	310	10	25,817
5	310	10	40,336
6	310	10	53,241
7	280	10	62,710
8	280	10	93,607
9	280	10	112,985
10	250	15	130,770
11	250	15	1,097,720
12	225	15	352,961
13	225	15	371,019
14	200	15	1,562,024
15	200	15	2,000,000
Steel Grade	**S690QL**		
Specimen Designation	**Stress Amplitude σ_a (MPa)**	**Frequency (Hz)**	**Number of Cycles to Failure N_f**
1	540	10	9857
2	540	10	11,227
3	540	10	8976
4	500	10	30,169
5	500	10	21,842
6	500	10	49,089
7	450	10	69,214
8	450	10	80,676
9	450	10	130,693
10	400	15	141,337
11	400	15	364,719
12	350	15	483,181
13	350	15	566,316
14	300	15	1,430,074
15	300	15	2,000,000
Steel Grade	**X37CrMoV5-1**		
Specimen Designation	**Stress Amplitude σ_a (MPa)**	**Frequency (Hz)**	**Number of Cycles to Failure N_f**
1	1000	10	10,613
2	1000	10	4025
3	1000	10	12,839
4	1000	10	12,280
5	800	10	87,089
6	800	10	12,554
7	800	10	95,546
8	600	15	38,035
9	600	15	58,871
10	600	15	25,192
11	600	15	70,825
12	600	15	51,055
13	500	15	164,237
14	500	15	2,110,777
15	500	15	2,583,827

The results of the experimental fatigue tests on smooth cylindrical specimens shown in Figure 5 for mild-strength S355J2+N, high-strength S690QL, and hot work tool steel grade X37CrMoV5-1 are displayed in Table 3. Table 3 summarizes the results of the fatigue tests carried out with smooth specimens under stress-controlled conditions. This table includes the controlled stress range; testing frequency; and the resulting number of cycles to failure, N_f, for each specimen. During the testing of specimens for S355J2+N and S690QL, the number of repeats was limited to two million cycles, and specimens with the designation of fifteen did not fail. For the testing of specimens for X37CrMoV5-1, the number of repeats was limited to five million cycles.

According to the experimental data shown in Table 3, the Basquin model described in Equation (1) and statistical analysis (linear model Y = A + BX, log-normal fatigue life distribution with constant variance along the entire interval of X used in testing) in accordance with standard ASTM E739-91 [43], the fatigue properties of the mild-strength S355J2+N steel, high-strength S690QL steel, and hot work tool steel grade X37CrMoV5-1 steel were determined and are shown in Table 4.

Table 4. Fatigue properties under uniaxial stress-controlled fully reversed testing, stress ratio $R = -1$.

Steel Grade	Fatigue Strength Coefficient $\sigma_{f'}$ (MPa)	Fatigue Strength Exponent b (-)
S355J2+N	1274.39	−0.1264
S690QL	1814.61	−0.1181
X37CrMoV5-1	6321.03	−0.1896

Based on uniaxial tension–compression stress-controlled experiments, the *S*–*N* curves (semi-log representation) for S355J2+N, S690QL, and X37CrMoV5-1 steel grades were determined and are shown in Figures 6–8, respectively, and combined in Figure 9.

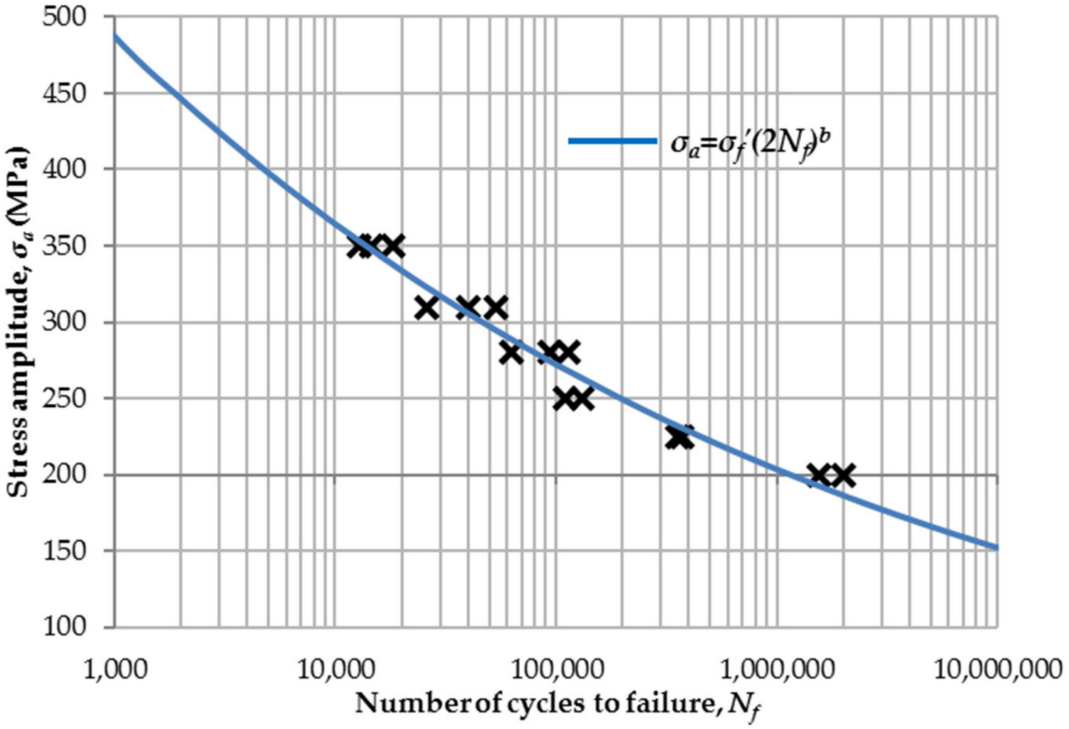

Figure 6. Semi-log *S*–*N* curve for uniaxial stress-controlled tests of S355J2+N steel grade.

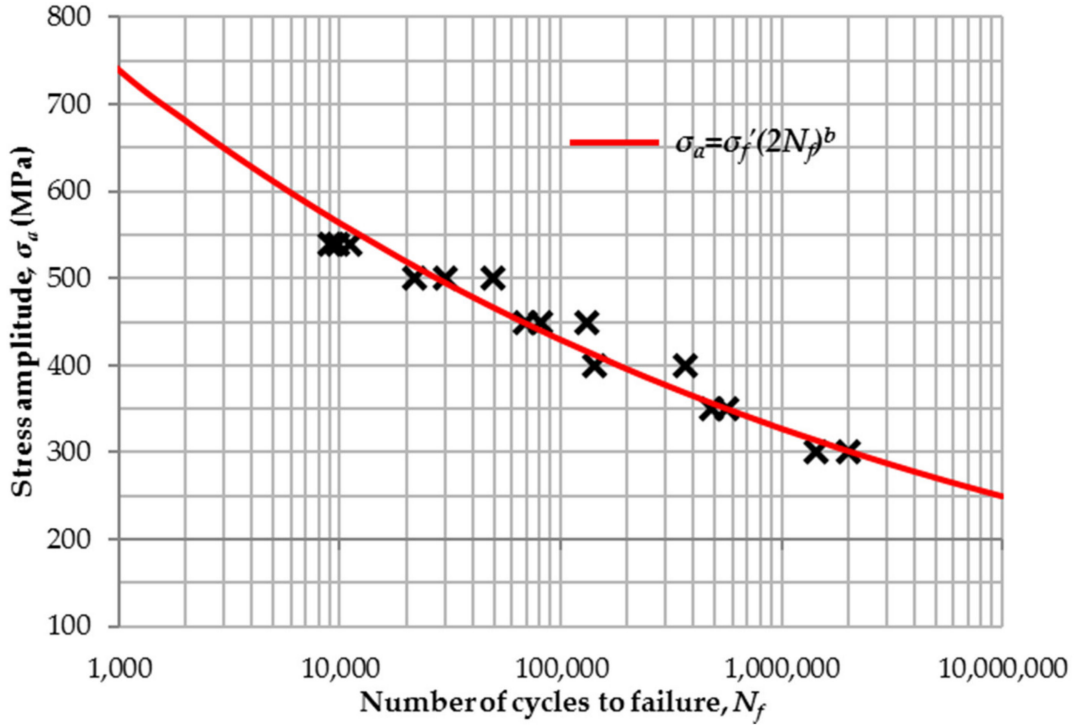

Figure 7. Semi-log *S*–*N* curve for uniaxial stress-controlled tests of S690QL steel grade.

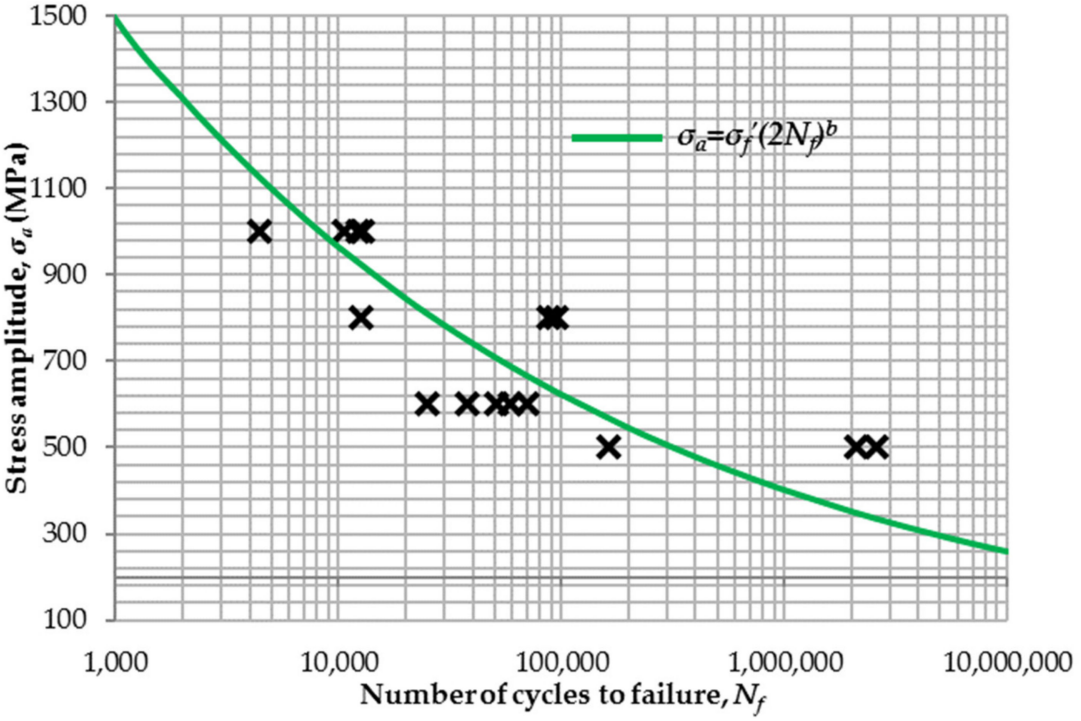

Figure 8. Semi-log *S*–*N* curve for uniaxial stress-controlled tests of X37CrMoV5-1 steel grade.

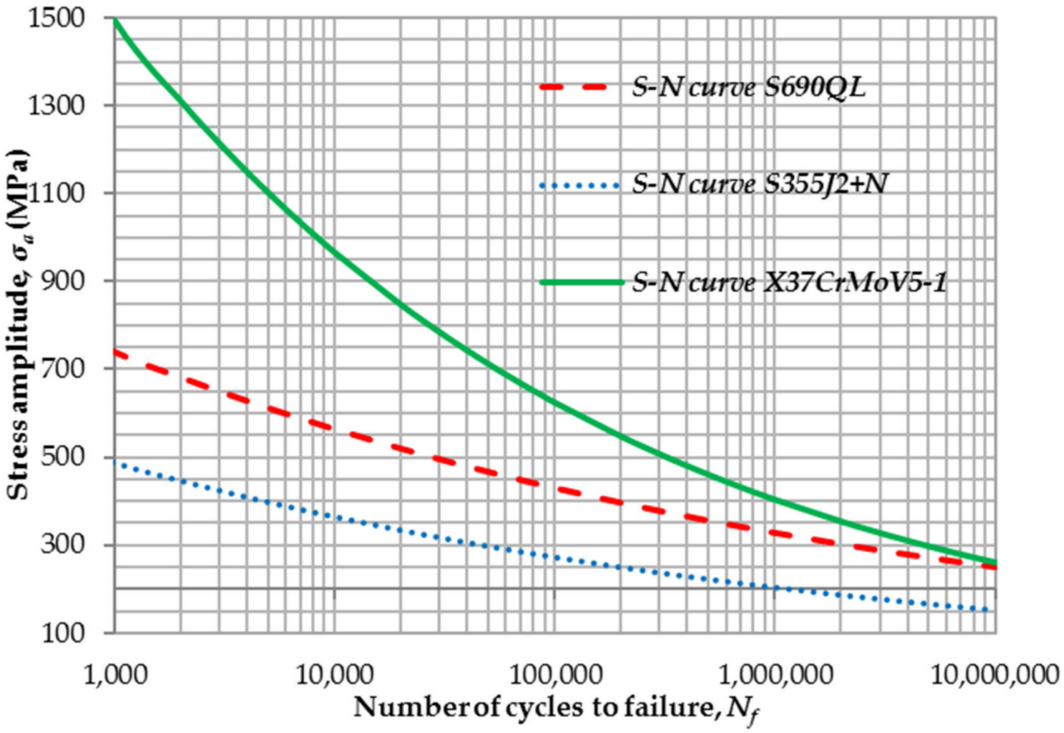

Figure 9. Combined diagram of semi-log *S–N* curves for S355J2+N, S690QL, and X37CrMoV5-1 steel grades.

4. Discussion

The stress–strain curves depicted in Figure 4 allow us to perform a comparison of the yield regions of all steel grades as well as the initial strain hardening behavior. It is clear that the S355J2+N steel shows a yield plateau, after which a very significant strain hardening can be verified. The S690QL steel does not show a yield plateau, and a relatively small strain hardening can be observed. When it comes to the X37CrMoV5-1 steel grade, from the diagram shown in Figure 4, it can be seen that it has extremely high tensile strength but very little maximum strain <2% due to its brittle nature caused by its martensitic structure. Such material behavior is common for hot work tool steels that need to be able to withstand high impact forces during operation without the occurrence of permanent deformations. However, if a critical force is reached and permanent deformations occur, the fracture of such steels occurs relatively quickly because the strain hardening is insignificant.

The reference value of the fatigue strength at N_C = 2 million cycles is denoted as $\Delta\sigma_c$, [13], and for the S355J2+N steel grade, its calculated value is about the same as class 160 of EN 1993-1-9 [13]. The results obtained for the S690QL steel grade show a fatigue behavior similar to that of the S355J2+N steel grade; however, the calculated $\Delta\sigma_c$ level of the S690QL steel grade is much higher than that of the S355J2+N value.

The best dynamic properties were certainly observed for the X37CrMoV5-1 steel grade. This steel grade has a high fatigue (endurance) limit, which was attained at about 500 MPa. The two tested samples achieved more than two million cycles, which is significantly more than the other two tested steel grades. For the X37CrMoV5-1 steel grade, the scattering of the results is somewhat higher than that in the other cases. The scattering of the results is most likely due to the high strength of the steel, the martensitic-carbide microstructure, and the large number of carbide inclusions of high hardness. However, based on the *S–N* curve, shown in Figure 8, the results can be clearly read. Such conclusions were somewhat expected given the tensile strength of the steel grade and its purpose.

Based on the visual examination of the fracture surfaces, it was determined that the steels S355J2+N and S690QL have a larger fatigue zone; i.e., for them, the time from the appearance of the initial crack to failure is longer than with the X37CrMoV5-1 steel.

Bearing in mind the mechanical characteristics of steel—above all, the ratio of strength to plasticity—such a conclusion was expected.

The visual examination of the fracture determined that the fracture that occurred in the S355J2+N and S690QL steels was assessed as predominantly ductile and the fracture of the X37CrMoV5-1 steel as predominantly brittle, which was expected considering the estimated structure of the steel.

5. Conclusions

The fatigue properties of mild-strength S355J2+N, high-strength S690QL, and hot work tool steel grade X37CrMoV5-1 were evaluated in this work. Some key points are listed below:

- The mild-strength S355J2+N steel was used as a reference point and was compared with S690QL and X37CrMoV5-1 steel.
- The fatigue behavior was investigated using uniaxial tension–compression stress-controlled experiments, with stress ratio $R = -1$, on smooth cylindrical specimens.
- Considering the high cycle fatigue regime and obtained S–N curves for all materials, the X37CrMoV5-1 steel grade showed superior fatigue behavior, and due to its yield strength, the X37CrMoV5-1 steel grade showed a higher endurance limit than the S355J2+N and S690QL steel grades at the same stress amplitudes.
- For the high cycle load, if we observe Basquin curves, the fatigue limit for the X37CrMoV5-1 steel grade tends to be similar to that of S690QL, even though these materials have very different stress–strain curves for the uniaxial tensile test.
- The X37CrMoV5-1 steel has a huge scattering of fatigue results, and it is very important to produce this steel under conditions as controlled as possible so that the structure is as uniform as possible.
- The utilization of high-strength steels increases the fatigue sensitivity of the construction components in comparison to components made of structural (mild-strength) steels because of the reduced cross-section and, consequently, increased stress.
- Therefore, such a new design would require verification using a numerical method, such as finite element analysis, and extensive experimental testing of the prototype [7], but the final product would have better quality and superior features.
- As a concluding remark, the design of construction components with high-strength steels (S690QL steel grade) should take advantage of the superior resistance of these steels to static and service (fatigue) loads.
- The S690QL steel grade has inferior fatigue properties to those of X37CrMoV5-1; however, it has much better weldability [12], and, therefore, it represents the optimum solution for designing lightweight, highly loaded constructions.

Author Contributions: Conceptualization, V.M. and D.A.; methodology, V.M.; software, M.Ž.; validation, D.A., M.T. and M.M.; formal analysis, M.M.; investigation, V.M. and D.A.; resources, M.Ž.; data curation, V.M. and M.T.; writing—original draft preparation, M.T.; writing—review and editing, V.M. and M.Ž.; visualization, M.M.; supervision, D.A.; project administration, V.M.; funding acquisition, M.Ž. and M.M. All authors have read and agreed to the published version of the manuscript.

Funding: This research was funded by the Ministry of Education, Science and Technological Development, Republic of Serbia, Grant TR32036, 451-03-68/2022-14/200378.

Institutional Review Board Statement: Not applicable.

Informed Consent Statement: Not applicable.

Data Availability Statement: Not applicable.

Conflicts of Interest: The authors declare no conflict of interest.

References

1. Stanford, N. Introducing *Alloys*: A Journal for Fundamental and Applied Research. *Alloys* **2022**, *1*, 1–2. [CrossRef]
2. Esha, E.; Hausmann, J. Development of an Analytical Model to Predict Stress–Strain Curves of Short Fiber-Reinforced Polymers with Six Independent Parameters. *J. Compos. Sci.* **2022**, *6*, 140. [CrossRef]
3. Tisza, M.; Czinege, I. Comparative Study of the Application of Steels and Aluminium in Lightweight Production of Automotive Parts. *Int. J. Lightweight Mater. Manuf.* **2018**, *1*, 229–238. [CrossRef]
4. Moynihan, M.C.; Allwood, J.M. Utilization of Structural Steel in Buildings. *Proc. R. Soc. A* **2014**, *470*, 20140170. [CrossRef]
5. Zhang, L. Prediction Method of Fatigue Crack Growth Life of High-Strength Steel for Industry 4.0. *IETE J. Res.* **2022**, 1–8. [CrossRef]
6. Milovanović, V.; Zivković, M.; Jovičić, G.; Kozak, D. The Analysis of Choice Influence in Fatigue Failure Criteria on Integrity Assessment of Wagon Structure. *Teh. Vjesn.* **2016**, *23*, 701–705. [CrossRef]
7. Correia, J.A.F.O.; da Silva, A.L.L.; Xin, H.; Lesiuk, G.; Zhu, S.-P.; de Jesus, A.M.P.; Fernandes, A.A. Fatigue Performance Prediction of S235 Base Steel Plates in the Riveted Connections. *Structures* **2021**, *30*, 745–755. [CrossRef]
8. Ho, H.C.; Chung, K.F.; Xiao, T.Y.; Yam, M.C.H.; Nethercot, D.A. Non-Linear Necking Behaviour of S275 to S960 Structural Steels under Monotonic Tension. *Eng. Struct.* **2022**, *261*, 114263. [CrossRef]
9. Guo, Y.B.; Ho, H.C.; Chung, K.F.; Elghazouli, A.Y. Cyclic Deformation Characteristics of S355 and S690 Steels under Different Loading Protocols. *Eng. Struct.* **2020**, *221*, 111093. [CrossRef]
10. Anandavijayan, S.; Mehmanparast, A.; Braithwaite, J.; Brennan, F.; Chahardehi, A. Material Pre-Straining Effects on Fatigue Behaviour of S355 Structural Steel. *J. Constr. Steel Res.* **2021**, *183*, 106707. [CrossRef]
11. Milovanović, V.; Dunić, V.; Rakić, D.; Živković, M. Identification Causes of Cracking on the Underframe of Wagon for Containers Transportation—Fatigue Strength Assessment of Wagon Welded Joints. *Eng. Fail. Anal.* **2013**, *31*, 118–131. [CrossRef]
12. Hu, Y.; Sun, C.; Xie, J.; Hong, Y. Effects of Loading Frequency and Loading Type on High-Cycle and Very-High-Cycle Fatigue of a High-Strength Steel. *Materials* **2018**, *11*, 1456. [CrossRef] [PubMed]
13. *EN 1993-1-9:2005*; Eurocode 3: Design of Steel Structures—Part 1-9: Fatigue. European Committee for Standardization: Brussels, Belgium, 2005.
14. *EN 13001-3-1:2012 + A2:2018*; Cranes—General Design—Part 3-1: Limit States and Proof Competence of Steel Structure. European Committee for Standardization: Brussels, Belgium, 2018.
15. Toasa Caiza, P.D.; Ummenhofer, T. A Probabilistic Stüssi Function for Modelling the S–N Curves and Its Application on Specimens Made of Steel S355J2+N. *Int. J. Fatigue* **2018**, *117*, 121–134. [CrossRef]
16. Spriestersbach, D.; Brodyanski, A.; Lösch, J.; Kopnarski, M.; Kerscher, E. Very High Cycle Fatigue of High-Strength Steels: Crack Initiation by FGA Formation Investigated at Artificial Defects. *Procedia Struct. Integr.* **2016**, *2*, 1101–1108. [CrossRef]
17. Glodež, S.; Knez, M.; Jezernik, N.; Kramberger, J. Fatigue and Fracture Behaviour of High Strength Steel S1100Q. *Eng. Fail. Anal.* **2009**, *16*, 2348–2356. [CrossRef]
18. Pijpers, R.J.M.; Kolstein, M.H.; Romeijn, A.; Bijlaard, F.S.K. Fatigue experiments on very high strength steel base material and transverse but welds. *Adv. Steel Constr.* **2009**, *5*, 14–32. [CrossRef]
19. Yin, G.-Q.; Kang, X.; Zhao, G.-P. Fatigue Properties of the Ultra-High Strength Steel TM210A. *Materials* **2017**, *10*, 1057. [CrossRef]
20. Yang, S.; Sun, J. Multiaxial Fatigue Life Assessment of 304 Austenitic Stainless Steel with a Novel Energy-Based Criterion. *Int. J. Fatigue* **2022**, *159*, 106728. [CrossRef]
21. Wei, H.; Liu, Y. An Energy-Based Model to Assess Multiaxial Fatigue Damage under Tension-Torsion and Tension-Tension Loadings. *Int. J. Fatigue* **2020**, *141*, 105858. [CrossRef]
22. Benedetti, M.; Berto, F.; Le Bone, L.; Santus, C. A Novel Strain-Energy-Density Based Fatigue Criterion Accounting for Mean Stress and Plasticity Effects on the Medium-to-High-Cycle Uniaxial Fatigue Strength of Plain and Notched Components. *Int. J. Fatigue* **2020**, *133*, 105397. [CrossRef]
23. Branco, R.; Prates, P.A.; Costa, J.D.; Berto, F.; Kotousov, A. New Methodology of Fatigue Life Evaluation for Multiaxially Loaded Notched Components Based on Two Uniaxial Strain-Controlled Tests. *Int. J. Fatigue* **2018**, *111*, 308–320. [CrossRef]
24. Ulewicz, R.; Szataniak, P.; Novy, F.; Trsko, L.; Bokuvka, O. Fatigue Characteristics of Structural Steels in the Gigacycle Region of Loading. *Mater. Today Proc.* **2017**, *4*, 5979–5984. [CrossRef]
25. Nový, F.; Petrů, M.; Trško, L.; Jambor, M.; Bokůvka, O.; Lago, J. Fatigue Properties of Welded Strenx 700 MC HSLA Steel after Ultrasonic Impact Treatment Application. *Mater. Today Proc.* **2020**, *32*, 174–178. [CrossRef]
26. Riccardo, G.; Rivolta, B.; Gorla, C.; Concli, F. Cyclic Behavior and Fatigue Resistance of AISI H11 and AISI H13 Tool Steels. *Eng. Fail. Anal.* **2021**, *121*, 105096. [CrossRef]
27. Dobrzański, L.A.; Polok, M.; Adamiak, M. Structure and Properties of Wear Resistance PVD Coatings Deposited onto X37CrMoV5-1 Type Hot Work Steel. *J. Mater. Process. Technol.* **2005**, *164–165*, 843–849. [CrossRef]
28. Pralea, B.; Nagit, G. Study of the Milling Tools When Machining X37CrMoV5-1 after Heat Treatment. *Procedia Manuf.* **2019**, *32*, 877–882. [CrossRef]
29. Zhang, Y.; Hu, C.L.; Zhao, Z.; Li, A.P.; Xu, X.L.; Shi, W.B. Low Cycle Fatigue Behaviour of a Cr–Mo–V Matrix-Type High-Speed Steel Used for Cold Forging. *Mater. Des.* **2013**, *44*, 612–621. [CrossRef]
30. Basquin, O.H. The Exponential Law of Endurance Tests. *Proc. ASTM* **1910**, *10*, 625–630.
31. Stephens, R.; Fatemi, A.; Stephens, R.; Fuchs, H. *Metal Fatigue in Engineering*; John Wiley & Sons Inc.: New York, NY, USA, 2001.

32. Manson, S.S. Discussion: "Experimental Support for Generalized Equation Predicting Low Cycle Fatigue". *J. Basic Eng.* **1962**, *84*, 537–541. [CrossRef]
33. Morrow, J. Cyclic Plastic Strain Energy and Fatigue of Metals. In *Internal Friction, Damping, and Cyclic Plasticity*; Lazan, B., Ed.; ASTM International: Montgomery, PA, USA, 1965; pp. 43–45. ISBN 9780803161603.
34. Mlikota, M.; Schmauder, S.; Božić, Ž. Calculation of the Wöhler (S–N) Curve Using a Two-Scale Model. *Int. J. Fatigue* **2018**, *114*, 289–297. [CrossRef]
35. Živković, J.; Dunić, V.; Milovanović, V.; Pavlović, A.; Živković, M. A Modified Phase-Field Damage Model for Metal Plasticity at Finite Strains: Numerical Development and Experimental Validation. *Metals* **2021**, *11*, 47. [CrossRef]
36. Lazić, V.; Aleksandrović, S.; Arsić, D.; Sedmak, A.; Ilić, A.; Đorđević, M.; Ivanović, L. The Influence of Temperature on Mechanical Properties of the Base Material and Welded Joint Made of Steel S690QL. *Metal.-Metall.* **2016**, *55*, 213–216.
37. Arsić, D.; Djordjević, M.; Zivković, J.; Sedmak, A.; Aleksandrović, S.; Lazić, V.; Rakić, D. Experimental-Numerical Study of Tensile Strength of the High-Strength Steel S690QL at Elevated Temperatures. *Strength Mater.* **2016**, *48*, 687–695. [CrossRef]
38. Arsić, D.; Lazić, V.; Sedmak, A.; Aleksandrović, S.; Živković, J.; Djordjević, M.; Mladenović, G. Effect of Elevated Temperatures on Mechanical Properties of Ultra High Strength Hot Work Tool Steel H11. *Trans. Famena* **2020**, *44*, 71–82. [CrossRef]
39. *EN ISO 6892-1:2011*; Metallic Materials—Tensile Testing—Part 1: Method of Test at Room Temperature. International Organization for Standardization: Geneva, Switzerland, 2011.
40. *ASTM: E8M-01*; Standard Test. Method for Tension Testing of Metalic Material. ASTM International: West Conshohocken, PA, USA, 2002.
41. *ASTM: E646-07*; Standard Test. Method for Tensile Strain-Hardening Exponents (n-Values) of Methalic Sheet Materials. ASTM International: West Conshohocken, PA, USA, 2007.
42. *ASTM: E468-90*; Standard Practice for Presentation on Constant Amplitude Fatigue Test Results for Metalic Materials. ASTM International: West Conshohocken, PA, USA, 2004.
43. *ASTM: E739-91*; Standard Practice for Statistical Analysis of Linear or Linearised Stress-Life (S–N) and Strain-Life (ε-N) Fatigue Data. ASTM International: West Conshohocken, PA, USA, 2004.